

Momentum Imbalance of Isolated Photon-Tagged Jet Production at RHIC and LHC

Wei Dai,¹ Ivan Vitev,² and Ben-Wei Zhang^{1,*}

¹*Key Laboratory of Quark & Lepton Physics (MOE) and Institute of Particle Physics,
Central China Normal University, Wuhan 430079, China*

²*Los Alamos National Laboratory, Theoretical Division, MS B238, Los Alamos, NM 87545, USA*
(Dated: May 21, 2018)

In collisions of ultra-relativistic nuclei, photon-tagged jets provide a unique opportunity to compare jet production and modification due to parton shower formation and propagation in strongly-interacting matter at vastly different center-of-mass energies. We present first results for the cross sections of jets tagged by an isolated photon to $\mathcal{O}(\alpha_{\text{em}}\alpha_s^2)$ in central Au+Au reactions with $\sqrt{s_{NN}} = 200$ GeV at RHIC and central Pb+Pb reactions with $\sqrt{s_{NN}} = 2.76$ TeV at LHC. We evaluate the increase in the transverse momentum imbalance of the observed γ +jet state, induced by the dissipation of the parton shower energy due to strong final-state interactions. Theoretical predictions to help interpret recent and upcoming experimental data are presented.

PACS numbers: 13.87.-a; 12.38.Mh; 25.75.-q

Hard parton scattering processes of $Q^2 \gg \Lambda_{\text{QCD}}^2$, such as the ones that produce energetic and/or massive hadronic final states at the world's premier collider facilities [1], have been widely used in the past decade to investigate the properties of the strongly-interacting quark-gluon plasma (QGP) created in ultra-relativistic heavy-ion collisions. Their utility as tomographic probes of the QGP [2] arises from the short interaction time $\sim 1/Q$ and the clear separation between the typical energy and momentum scales that characterize the probe and the medium [3]. Among such hard probes, large transverse momentum jets [4, 5] have recently emerged as a new tool, which not only provides the most promising channel to test and advance perturbative Quantum Chromodynamics (QCD) in the many-body environment of ultra-relativistic nuclear collisions, but is also more sensitive to the details of the in-medium parton shower dynamics than leading hadron production [6, 7].

Jets tagged by photons (γ) or electroweak bosons (W^\pm , Z^0) are particularly well suited to studying heavy-ion collisions [8, 9] since the tagging particle escapes the region of strongly-interacting matter unscathed. For example, the CMS collaboration measurements in lead-lead (Pb+Pb) collisions show absence of significant modification of high transverse momentum photon production relative to the binary collision-scaled proton-proton (p+p) result within the current statistical and systematic uncertainties [10]. Thus, in the collinear factorization approach γ s can provide, on average, constraints on the energy of the away-side parton shower [11]. Furthermore, jets tagged by photons or electroweak bosons are largely unaffected by the fluctuations of the soft hadronic background [9] that may complicate the interpretation of di-jet modification in heavy-ion collisions [12–14]. By selecting a suitable range for the transverse momentum of the tagging photon (p_{T_γ}), accessible at both RHIC and LHC, the in-medium modification of parton showers in dense matter created at very different $\sqrt{s_{NN}}$ can be studied. In the jet suppression region, where the trans-

verse momentum of the jet $p_{T_{\text{jet}}} \geq p_{T_\gamma}$, the attenuation of photon-tagged jets and inclusive jets [15] can be directly compared.

In addition to being theoretically attractive, the γ +jet channel is being actively investigated by the LHC experiments. Recently, the ATLAS collaboration reported progress in the measurement of photon+jet production cross sections in p+p collisions at $\sqrt{s} = 7$ TeV [16]. The CMS collaboration observed a significant enhancement in the transverse momentum imbalance of photon-tagged jet events central Pb+Pb reactions at $\sqrt{s_{NN}} = 2.76$ TeV, providing a direct quantitative measure of parton energy loss in the QCD medium [17]. Photon-tagged jet results are also expected in the near future from RHIC experiments at much lower $\sqrt{s_{NN}}$.

With this motivation, we present theoretical predictions for the cross section modification and the growth in the transverse momentum imbalance of photon-tagged jet events in heavy ion collisions at RHIC and LHC. Our results combine the $\mathcal{O}(\alpha_{\text{em}}\alpha_s^2)$ perturbative cross sections with initial-state cold nuclear matter effects and final-state parton shower modification and energy dissipation in the QGP.

The cross section for prompt photon production is given by the sum of its direct and fragmentation contributions and can be written schematically as [18, 19]:

$$d\sigma^\gamma = d\sigma^{(D)}(\mu_R, \mu_f) + \sum_{k=q,\bar{q},g} d\sigma_k^{(F)}(\mu_R, \mu_f, \mu_{fr}) \otimes D_{\gamma/k}(\mu_{fr}), \quad (1)$$

Here, $\sigma^{(D)}$ (direct), $\sigma^{(F)}$ (fragmentation) are the corresponding cross sections for a photon or a parton and $D_{\gamma/k}(\mu_{fr})$ is the fragmentation function of parton k into a photon. In Eq. (1) μ_R, μ_f, μ_{fr} are the renormalization, factorization and fragmentation scales, respectively. We denote by \otimes the standard convolution over the fragmentation momentum fraction. In this paper we take advantage of JETPHOX [18], a Monte Carlo program

designed to calculate $p + p \rightarrow \gamma/h + J + X$. For inclusive γ/h production it yields next-to-leading (NLO) order accuracy. For the more differential $\gamma + \text{jet}$ channel the $\mathcal{O}(\alpha_{\text{em}}\alpha_s^2)$ evaluation gives the leading cross section contribution away from $p_{T_\gamma} \approx p_{T_{\text{jet}}}$.

TeV collider experiments, such as CDF and D0 at the Tevatron, ATLAS and CMS at LHC, implement constraints on the hadronic activity that accompanies photon candidate events. By imposing an upper limit on the hadronic transverse energy in a given cone of radius $R_{\text{iso.}} = \sqrt{(y - y_\gamma)^2 + (\phi - \phi_\gamma)^2}$ around the photon direction, the cross section for isolated photons can be obtained. The isolation cut not only rejects the background of secondary photons coming from several decay channels, but also affects the prompt photon cross section itself by reducing the contributions of the fragmentation component [19]. Here, we will focus on jets tagged by isolated photons.

Measurements of the production cross section of isolated photons associated with jets in proton-antiproton ($p + \bar{p}$) collisions at $\sqrt{s} = 1.96$ TeV were performed by the D0 collaboration at the Tevatron [20]. The baseline simulation in “elementary” nucleon-nucleon interactions can be validated against the experimental results, as shown in Fig. 1. Here, the differential cross section of the final state photon $d^3\sigma/dy_\gamma dy_{\text{jet}} dp_{T_\gamma}$ is given for specific transverse momentum and rapidity cuts for the leading away-side jet. We consider kinematic regions around mid rapidity $|y^\gamma| < 1.0$, $|y^{\text{jet}}| < 0.8$. The transverse momentum cuts are: $p_{T_\gamma} > 30$ GeV, $p_{T_{\text{jet}}} > 15$ GeV. Our theoretical simulation employs the CTEQ 6.6 parton distribution functions and the BGF II fragmentation functions [18]. All scales are chosen to be $\mu_{R,f,f_r} = p_{T_\gamma} \sqrt{(1 + \exp(-2|y^*|)/2)}$, with $y^* = 0.5(y_\gamma - y_{\text{jet}})$. To compare to the D0 results, we implement a midpoint cone algorithm with a radius parameter $R = 0.7$ for the jet and impose an isolation cut that requires the hadronic transverse energy in the cone of radius $R_{\text{iso.}} = 0.4$ around the photon direction to be less than 7% of the γ energy. We find that the theoretical predictions provided by JETPHOX are in good agreement with the measured cross section within the statistical and systematic uncertainties for either equal ($y_\gamma y_{\text{jet}} > 0$) or different ($y_\gamma y_{\text{jet}} < 0$) signs of the jet and photon rapidities. The bottom panel of Fig. 1 shows the fractional deviation (Data-Theory)/Theory.

In reactions with heavy nuclei, cold nuclear matter (CNM) effects prior to the QGP formation, such as initial-state energy loss, power corrections and the Cronin effect, can modify the experimentally observed photon+jet cross sections. At RHIC and LHC we are interested in jets of $p_{T_{\text{jet}}} > 10$ GeV or 30 GeV, respectively. At these energy scales only initial-state energy loss may play a role [14, 21]. As we will see below, the CNM effects do not affect the asymmetry of photon+jet events. The suppression of photon+jet production, induced by CNM

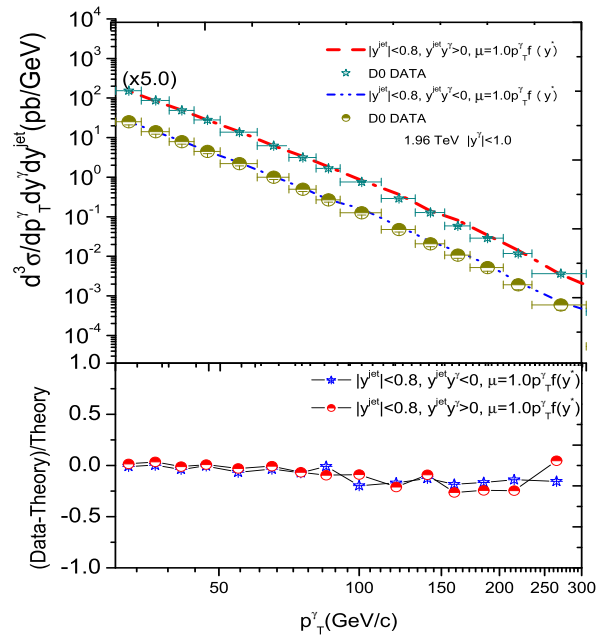


FIG. 1: Comparison between the isolated photon+jet cross section measured by the D0 experiment and the $\mathcal{O}(\alpha_{\text{em}}\alpha_s^2)$ pQCD theory in $p + \bar{p}$ collisions at $\sqrt{s_{NN}} = 1.96$ TeV.

effect, is fairly small. Final-state quark-gluon plasma effects include radiative energy loss, caused by medium-induced parton splitting [21], and the dissipation of the energy of the parton shower through collisional interactions in the strongly-interacting matter [22]. To evaluate the isolated photon+jet cross section, we use the theoretical framework of [6, 15], which clearly outlines the similarities and differences between jet and leading particle production in the ambiance of the QGP. The medium-modified photon+jet cross section per binary scattering is calculated as follows:

$$\frac{1}{\langle N_{\text{bin}} \rangle} \frac{d\sigma^{AA}}{dp_{T_\gamma} dp_{T_{\text{jet}}}} = \sum_{q,g} \int_0^1 d\epsilon \frac{P_{q,g}(\epsilon)}{1 - [1 - f(R)]\epsilon} \times R_{q,g} \frac{d\sigma^{\text{CNM}}\left(p_{T_\gamma}, \frac{p_{T_{\text{jet}}}}{1 - [1 - f(R)]\epsilon}\right)}{dp_{T_\gamma} dp_{T_{\text{jet}}}}. \quad (2)$$

The $\gamma + \text{jet}$ production points are distributed according to the binary nucleon-nucleon collision density and propagate through the medium that follows the participant number density and undergoes Bjorken expansion. The properties of the gluon-dominated medium are related to the local temperature: $m_D = g_{\text{med}}T$, $\sigma^{gg} = \lambda = 1/(\sigma^g g\rho)$ In Eq. (2) $P_{q,g}(\epsilon)$ is the probability distribution that a fraction ϵ of the hard-scattered quark or gluon energy is converted to a medium-induced parton shower [6, 8] and $R_{q,g}$ is the fraction of the corresponding hard-scattered partons. Part of the dependence of the jet cross section on the jet reconstruction parameters, such as the radius R , is contained in $d\sigma^{\text{CNM}}/dp_{T_\gamma} dp_{T_{\text{jet}}}$. More importantly, the fraction of

the parton shower energy that is simply redistributed inside the jet due to final-state interactions $f(R)$ also depends on R [$f(R)_{R \rightarrow 0} \rightarrow 0$, $f(R)_{R \gg 1} \rightarrow 1$] [6, 13, 15]. In our calculation $P_{q,g}(\epsilon)$ and $f(R)$ are evaluated on an event-per-event basis. The physics meaning of Eq. (2) is that the observed photon-tagged jet cross section in nucleus-nucleus reactions is a probabilistic superposition of cross sections where the jet is of higher initial transverse momentum $p_{T_{\text{jet}}}/\{1 - [1 - f(R)]\epsilon\}$.

The many-body QCD dynamics that modifies isolated photon + jet production in relativistic heavy-ion collisions is manifested in the deviation from the baseline p+p results, scaled by the number of binary nucleon-nucleon interactions $\langle N_{bin} \rangle$ [6, 9]:

$$R_{AA}^{\gamma\text{-jet}}(p_{T_{\text{jet}}}, p_{T_{\gamma}}; R) = \frac{\frac{d\sigma^{AA}}{dp_{T_{\gamma}} dp_{T_{\text{jet}}}}}{\langle N_{bin} \rangle \frac{d\sigma^{pp}}{dp_{T_{\gamma}} dp_{T_{\text{jet}}}}} . \quad (3)$$

Theoretical predictions for the nuclear modification of the photon+jet production rate are presented in Fig. 2, where we show $R_{AA}^{\text{jet}}(p_{T_{\text{jet}}}; R)$ with the tagging γ momentum integrated in the region $32.5 < p_{T_{\gamma}} < 37.5$ GeV. We choose a jet reconstruction radius $R=0.3$ and give results for central Au+Au collisions at RHIC (solid line) central Pb+Pb collisions at LHC (dashed line). We note direct comparison between RHIC and LHC is possible for the first time in a more exclusive channel. The largest suppression is observed for $p_{T_{\text{jet}}} \approx p_{T_{\gamma}}$ and for $p_{T_{\text{jet}}} > p_{T_{\gamma}}$ $R_{AA}^{\gamma\text{-jet}} < 1$. In the presented transverse momentum range the suppression at LHC is slightly larger even though the jet spectra are harder, reflective of higher temperature, density and stopping power of the QGP at LHC. Bands represent a range of couplings between the jet and the medium $g_{\text{med}} = 1.8 - 2.2$. For $p_{T_{\text{jet}}} < p_{T_{\gamma}}$ there can be a strong enhancement of the cross section. In the studied transverse momentum range this is the case at RHIC and it reflects the narrower baseline jet distribution away from $p_{T_{\text{jet}}} \approx p_{T_{\gamma}}$ due to the smaller \sqrt{s} . Fig. 2 illustrates the flexibility that photon-tagged afford in comparing the properties of deconfined strongly-interacting matter at RHIC and LHC.

Let us define by $z_{J\gamma} = p_{T_{\text{jet}}}/p_{T_{\gamma}}$ the momentum imbalance of photon+jet events. Its distribution can be obtained from the $\mathcal{O}(\alpha_{\text{em}}\alpha_s^2)$ double differential cross section $d\sigma/dp_{T_{\gamma}} dp_{T_{\text{jet}}}$. By changing variables from $(p_{T_{\gamma}}, p_{T_{\text{jet}}})$ to $(z_{J\gamma}, p_{T_{\text{jet}}})$ and integrating over $p_{T_{\text{jet}}}$, we can express:

$$\frac{d\sigma}{dz_{J\gamma}} = \int_{p_{T_{\text{jet}}}^{\text{min}}}^{p_{T_{\text{jet}}}^{\text{max}}} dp_{T_{\text{jet}}} \frac{p_{T_{\text{jet}}}}{z_{J\gamma}^2} \frac{d\sigma[z_{J\gamma}, p_{T_{\gamma}}(z_{J\gamma}, p_{T_{\text{jet}}})]}{dp_{T_{\gamma}} dp_{T_{\text{jet}}}} . \quad (4)$$

Here, $p_{T_{\text{jet}}}^{\text{min}}$, $p_{T_{\text{jet}}}^{\text{max}}$ can be specified by the experiment and together with the transverse momentum cuts on the isolated photons contribute to the shape of the $z_{J\gamma}$ distribution. In our p+p and Pb+Pb calculations at LHC we use the CMS experimental cuts $p_{T_{\text{jet}}} > 30$ GeV,

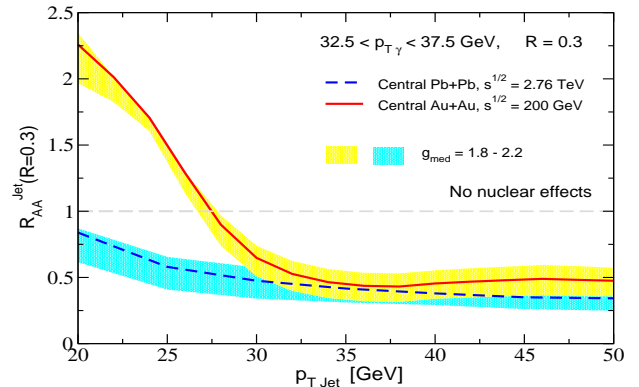


FIG. 2: The nuclear modification factor $R_{AA}^{\gamma\text{-jet}}$ for the isolated photon-tagged jets in the most central A+A reactions at RHIC and LHC ($R=0.3$).

$p_{T_{\gamma}} > 60$ GeV, $|y^{\gamma}| < 1.44$, $|y^{\text{jet}}| < 1.6$, $|\phi^{\text{jet}} - \phi^{\gamma}| > \frac{7}{8}\pi$. We implement a k_T algorithm with a radius parameter $R = 0.3$ for the jet and isolation criterion that requires the total energy within a cone of radius $R_{\text{iso}} = 0.4$ surrounding the photon direction to be less than 5 GeV. In p+p and Au+Au collisions at RHIC, we consider the same cuts except $p_{T_{\text{jet}}} > 10$ GeV, $p_{T_{\gamma}} > 30$ GeV, and impose a different isolation cut that requires the hadronic transverse energy in the cone of radius $R_{\text{iso}} = 0.4$ around the photon direction to be less than 7% of the γ energy.

The normalized momentum imbalance distribution $(1/\sigma)d\sigma/dz_{J\gamma}$ is given in Fig. 3. The solid black line shows the p+p calculation and the circles represent the CMS result with large error bars. The dotted cyan line includes cold nuclear matter effects in central Pb+Pb (top panel) and central Au+Au (bottom panel) reactions at LHC and RHIC, respectively. These CNM effects do not affect the $z_{J\gamma}$ distribution appreciably. The physics responsible for the difference between p+p and A+A reactions is then contained in the final-state QGP-induced parton splitting and the dissipation of the parton shower energy in the medium. The parameter that controls the strength of the coupling between the jet constituents and the strongly interacting matter is g_{med} . We investigate a range of values $g_{\text{med}} = 1.8$ (green dashed), 2.0 (blue dot-dashed), 2.2 (red short dot-dashed) that has worked well in describing the di-jet asymmetry distribution and in predicting the inclusive jet suppression at LHC [13]. The same range of coupling strengths has been used to predict the asymmetry distribution of Z^0 +jet events in heavy-ion collisions [9].

The effect of final-state interactions is to broaden the momentum imbalance distribution and shift it down to smaller values of $z_{J\gamma}$. Our calculations include both radiative and collisional energy losses that alter the associated jet transverse momentum. They differ in the amount of shift observed, but the broadening is approximately independent of the value of g_{med} . It should be noted that even in p+p collisions the distribution peaks

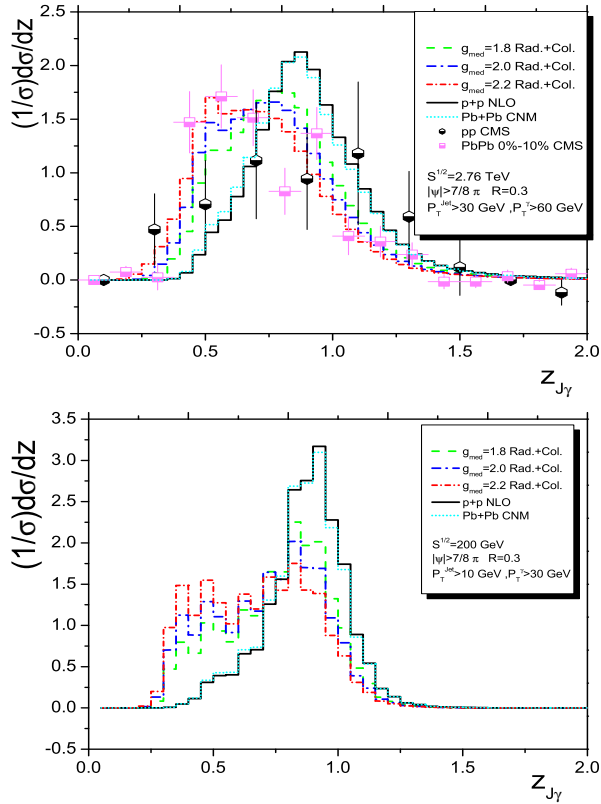


FIG. 3: The isolated photon-tagged jet asymmetry distribution for different coupling strengths between the jet and the medium. Top panel: Pb+Pb collisions at $\sqrt{s_{NN}} = 2.76$ TeV. Black and magenta points are CMS experimental data in p+p and Pb+Pb collision, respectively. Bottom panel: Au+Au collisions at $\sqrt{s_{NN}} = 200$ GeV.

below $z_{J\gamma} = 1$. We define the mean value of $z_{J\gamma}$ as:

$$\langle z_{J\gamma} \rangle = \int dz_{J\gamma} z_{J\gamma} \frac{1}{\sigma} \frac{d\sigma}{dz_{J\gamma}}, \quad (5)$$

and show its values in Table I. The steeper falling cross sections at RHIC energies lead not only to a narrower $z_{J\gamma}$ distribution in p+p collisions but also to larger broadening end shift in $\langle z_{J\gamma} \rangle$ in A+A collisions in spite of the fact that, on average, less energy per jet is dissipated as the parton shower forms and propagates in the QGP. Our results, quoted in Table I, can also be compared directly to the most central Pb+Pb data, where CMS measured the ratio $\langle z_{J\gamma} \rangle = 0.73 \pm 0.02(\text{stat.}) \pm 0.04(\text{syst.})$ [23].

In summary, we presented first results for the differential cross sections and momentum imbalance of isolated photon-tagged jets in p+p and A+A collisions at RHIC and LHC. We found that a theoretical approach that combines the $\mathcal{O}(\alpha_{em}\alpha_s^2)$ perturbative cross sections with the medium-induced parton splitting and parton shower energy dissipation in the QGP describes quantitatively the increase of the transverse momentum imbalance observed by the CMS experiment in central Pb+Pb reactions at $\sqrt{s_{NN}} = 2.76$ TeV. Through comparison between

TABLE I: Theoretical results for $\langle z_{J\gamma} \rangle$ in p+p, central Pb+Pb and central Au+Au reactions. Center-of-mass energies are: LHC $\sqrt{s_{NN}} = 2.76$ TeV, RHIC $\sqrt{s_{NN}} = 200$ GeV.

System	$\langle z_{J\gamma} \rangle_{\text{LHC}}$	$\langle z_{J\gamma} \rangle_{\text{RHIC}}$
p+p	0.94	0.90
A+A, CNM	0.94	0.89
A+A, $g_{med} = 1.8$, Rad.+Col.	0.84	0.78
A+A, $g_{med} = 2.0$, Rad.+Col.	0.80	0.74
A+A, $g_{med} = 2.2$, Rad.+Col.	0.71	0.70

theoretical predictions, such as the modification of the γ +jet cross sections and the associated $z_{J\gamma}$ distribution presented here, and upcoming experimental results, the emerging picture of in-medium parton shower formation and evolution can further be tested at RHIC and LHC.

* Electronic address: bwzhang@iopp.cnu.edu.cn

- [1] J. F. Owens, Rev. Mod. Phys. **59**, 465 (1987).
- [2] X.-N. Wang and M. Gyulassy, Phys. Rev. Lett. **68**, 1480 (1992).
- [3] G. Ovanessian and I. Vitev, JHEP **1106**, 080 (2011).
- [4] G. Sterman, S. Weinberg, Phys. Rev. Lett. **39**, 1436 (1977).
- [5] S. D. Ellis, Z. Kunszt and D. E. Soper, Phys. Rev. Lett. **64**, 2121 (1990).
- [6] I. Vitev, S. Wicks and B. W. Zhang, JHEP **0811**, 093 (2008);
- [7] T. Renk, Phys. Rev. C **80**, 044904 (2009).
- [8] R. B. Neufeld, I. Vitev, B.-W. Zhang, Phys. Rev. **C83**, 034902 (2011).
- [9] R. B. Neufeld and I. Vitev, Phys. Rev. Lett. **108**, 242001 (2012).
- [10] CMS Collaboration, Phys. Lett. B **710**, 256 (2012).
- [11] X.-N. Wang, Z. Huang, and I. Sarcevic, Phys. Rev. Lett. **77**, 231 (1996).
- [12] M. Cacciari, G. P. Salam and G. Soyez, Eur. Phys. J. C **71**, 1692 (2011).
- [13] Y. He, I. Vitev and B. -W. Zhang, Phys. Lett. B **713**, 224 (2012).
- [14] Y. He, B.-W. Zhang, E. Wang, Eur. Phys. J. C **72** 1904 (2012).
- [15] I. Vitev and B. W. Zhang, Phys. Rev. Lett. **104**, 132001 (2010).
- [16] G. Aad *et al.* [ATLAS Collaboration], Phys. Rev. D **85**, 092014 (2012).
- [17] S. Chatrchyan *et al.* [CMS Collaboration], Phys. Lett. B **710**, 256 (2012).
- [18] S. Catani, M. Fontannaz, J.P. Guillet, E. Pilon. JHEP **0205**, 028 (2002).
- [19] Z. Belghobsi, M. Fontannaz, J.-Ph. Guillet, *et al.*, Phys. Rev. D **79**, 114024 (2009).
- [20] V.M. Abazov *et al.* [D0 Collaboration], Phys. Lett. B **666**, 435(2009).
- [21] I. Vitev, Phys. Rev. **C75**, 064906 (2007).
- [22] R. B. Neufeld and I. Vitev, Phys. Rev. C **86**, 024905 (2012); R. B. Neufeld, Phys. Rev. D **83**, 065012 (2011).
- [23] S. Chatrchyan *et al.* [CMS Collaboration], Phys. Lett. B **718**, 773 (2013).